Electric-field-induced B_1-B_2 transition in bent-core mesogens

J. Ortega,[1,][*] M. R. de la Fuente,[1] J. Etxebarria,[2] C. L. Folcia,[2] S. Díez,[1] J. A. Gallastegui,[2] N. Gimeno,[3] M. B. Ros,[3] and M. A. Pérez-Jubindo[1]

[1]*Departamento de Física Aplicada II, Facultad de Ciencias, Universidad del País Vasco, Apartado 644, 48080 Bilbao, Spain*
[2]*Departamento de Física de la Materia Condensada, Facultad de Ciencias, Universidad del País Vasco, Apartado 644, 48080 Bilbao, Spain*
[3]*Departamento de Química Orgánica, Facultad de Ciencias–ICMA, Universidad de Zaragoza–CSIC, 50009 Zaragoza, Spain*

We report experimental results on two bent-shaped mesogens showing the B_1 phase. Contrary to the conventional B_1 structures, we have found that our compounds display a clear electro-optic effect in this phase. Under the influence of a 100-Hz square-wave electric field of moderate amplitude, an increase of the birefringence is observed. However, no switching current is detected, indicating that the materials remain antiferroelectric. For high enough fields, a drastic change in the texture occurs. This change is a phase transition to a B_2 phase, and shows the typical antiferroelectric switching of this phase. The induced B_2 phase has been identified to be homochiral. Upon removal of the field, the B_1 structure is recovered. Our study is based on differential scanning calorimetry, x-ray, electro-optics, polarization reversal, and dielectric measurements.

I. INTRODUCTION

Bent-core molecules, due to their special shape, pack forming lamellar structures with an in-layer polar order [1,2]. The simplest mesophase in this kind of materials is the B_2 phase [2,3], which is a smectic structure with an antiferroelectric arrangement of the electric dipoles in neighboring layers [Fig. 1(a)]. This mesophase is found in molecules with relatively long aliphatic chains, and is supposed to be brought about by the tendency of the aromatic cores to segregate from the terminal chains. As the length of the chains is decreased, the materials have an alternative route to avoid bulk spontaneous polarization, tending to form the B_1 phase [2,4]. In this structure [Figs. 1(b) and 1(b$'$)] [5], the chains of the molecules of one domain overlap with the cores of the molecules of the neighboring domain at the interfaces between domains. The structure is stabilized by the competition of the core-core attraction and the core-chain segregation at these interfaces. If the chain length is reduced further, the B_6 phase appears [Fig. 1(c)], which is a lamellar structure with intercalated molecules [2,8]. The intercalation can occur because the unfavorable core-chain interaction is small in this case, whereas the entropy of this phase is larger than that of the B_1 phase.

This scheme for the successive appearance of the different structures in a homologous series of bent-core molecules is well followed in practice [9,10]. Usually the materials present only one of the referred mesophases, though in a few cases a B_6-B_1 dimorphism is found [8]. Curiously, however, the B_1-B_2 sequence is extremely rare. In fact, we have found only one material in the literature where both phases appear both on heating and cooling [11]. Therefore, it seems of interest to present more examples of this phase transition. In this paper, we will study one new compound with this phase sequence. In addition, we will see with two examples that the

B_1-B_2 transition can also be induced by an electric field. This phenomenon has not been observed up to now.

II. MATERIALS AND EXPERIMENTAL TECHNIQUES

The chemical structures together with the phase sequence of the studied materials are shown in Fig. 2. The synthesis of the compounds will be reported elsewhere. The identification of the different phases will be explained below. The materials were investigated by means of several techniques: differential scanning calorimetry (DSC), optical microscopy, x-ray scattering, spontaneous polarization, and dielectric measurements. For the optical, polarization, and dielectric studies, commercial glass cells were used (Linkam, with thickness $d=5$ μm and EHC, with $d=7$ μm). The x-ray measurements were carried out on unaligned samples in capillary tubes.

III. STUDY OF THE HIGH-TEMPERATURE MESOPHASES

We will first present our characterization studies of the high-temperature mesophases of compounds 1 and 2. These phases were identified as B_1 and the identification was based on the following evidence.

(i) The textures obtained on slow cooling from the isotropic liquid [Figs. 3(a) and 3(b)] are of the so-called mosaic type, which are typical of the B_1 phase.

(ii) The low-angle x-ray reflections can be successfully indexed under the hypothesis of a columnar centered rectangular (B_1) phase (see Table I). The c parameter in both materials is compatible with the molecular length deduced theoretically by molecular modeling, assuming a bending angle of 120° and an all-*trans* conformation for the aliphatic chains. The deduced molecular lengths are somewhat larger, $L=63$ and 65 Å for compounds 1 and 2, respectively, which could mean a certain degree of interdigitation, smaller bending angles, or disorder in the terminal chains [12]. In the high-angle region, a diffuse ring is also observed in both

*Email address: wmporapj@lg.ehu.es
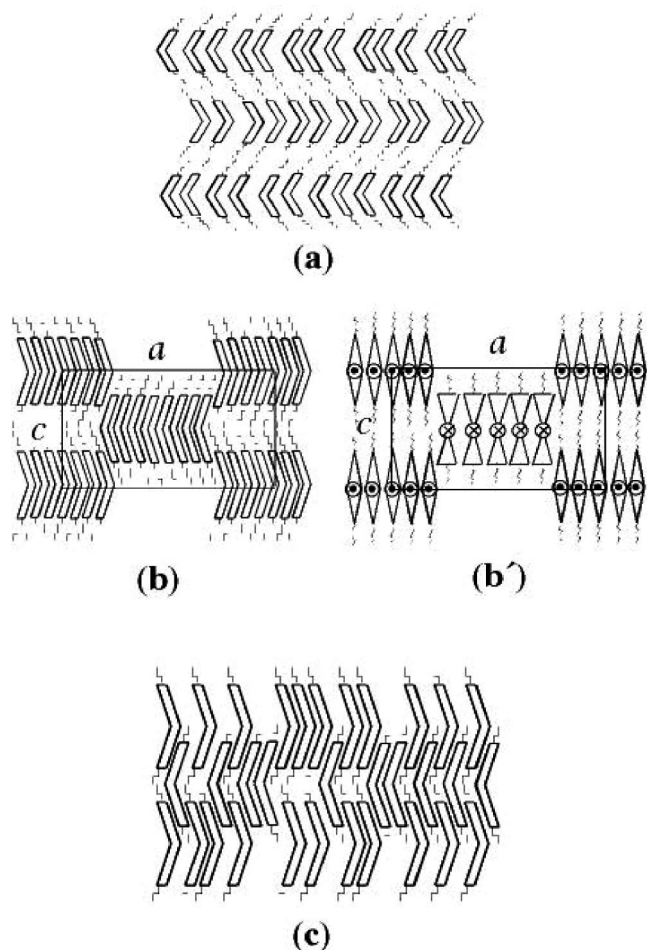
FIG. 1. Schematic representation of the molecular arrangements in phases (a) B_2, (b) and (b′) B_1, and (c) B_6. For simplicity, the molecular tilt in the B_2 phase has been omitted.

Compound 1

I-156.7 (20.2)-**B$_1$**-120.3 (0.45)-**B$_2$**-83.3 (13.9)-**K**
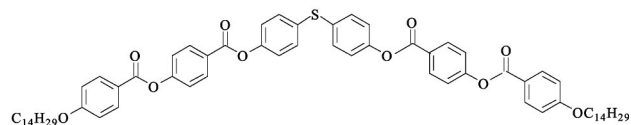
Compound 2

I-155.8 (26.1)- **B$_1$**-150.1 (22.5)-**K**-128.1 (23.5)-**K′**

FIG. 2. Chemical structure and phase sequences on cooling of the studied compounds. I, K, and $K′$ represent isotropic and two different crystalline phases, respectively. The transition enthalpies appear in brackets and are expressed in kJ/mol. The transition temperatures correspond to those obtained by DSC measurements.

cases, corresponding to a liquid disorder in the columns with an average molecular distance of 4.6 Å. The a parameter then corresponds to a number of molecules in the cross section of the column of about 9 for both compounds.

The optical textures can be interpreted even more quantitatively. First, some circular domains (or at least part of them) are clearly visible both in Figs. 3(a) and 3(b), where the extinction brushes are oriented along the polarizer and analyzer directions. This indicates an orthogonal phase [14], compatible with the B_1 structure. On the other hand, the different colors of the textures can be explained as due to different birefringence values Δn because of the different molecular orientations [15]. More specifically, in compound 1 the colors vary from purple ($\Delta n_{min}=0.11$) to green ($\Delta n_{max}=0.16$), and in compound 2 the highest Δn value is $\Delta n_{max}=0.13$ (blue) and the smallest $\Delta n_{min}=0.08$ (yellow). These data were checked with a compensator. Δn_{max} corresponds to a molecular orientation where the dipole is perpendicular to the cell plates, whereas Δn_{min} is for the molecular plane nearly parallel to the plates. The molecules can be modeled by means of two uniaxial wings (Fig. 4) with ordinary and extraordinary refractive indices typical of calamitic molecules ($n_o=1.5$, $n_e=1.7$), and with a bending angle β.

Assuming a β value of 124° for compound 1 and 115° for compound 2, the correspondence with the experimental maximum and minimum Δn values is fairly good. All these parameters seem reasonable. The values of the calculated principal indices and birefringence together with the experimental birefringence are indicated in Fig. 4.

Now, contrary to the commonly observed B_1 structures, the phases of these compounds do respond to the electric field. Figures 3(c) and 3(d) show the texture transformation under a square-wave field of amplitude 15 V/μm and frequency $\nu=100$ Hz. In both cases, the variety of colors disappears, leaving only a uniform color that corresponds to the maximum Δn. This means that all the electric dipoles in the sample orient in a direction perpendicular to the cell plates. However, there is no polarization switching current, which indicates that the alignment of dipoles is an effect probably due to the dielectric anisotropy of the materials and is quadratic in the field. The materials therefore remain antiferroelectric. The effect is partially reversible, i.e., some of the original colors are restored when the field is removed. This is especially the case for compound 1.

In principle, all these texture observations would be compatible with the B_1 reversed (B_{1rev}) phase [Fig. 1(b′)] [16]. The B_{1rev} phase has also been proposed for a dimeric compound where birefringence changes have been found under an applied electric field [17]. A definitive proof of how the molecular orientation is could be given by means of x-ray
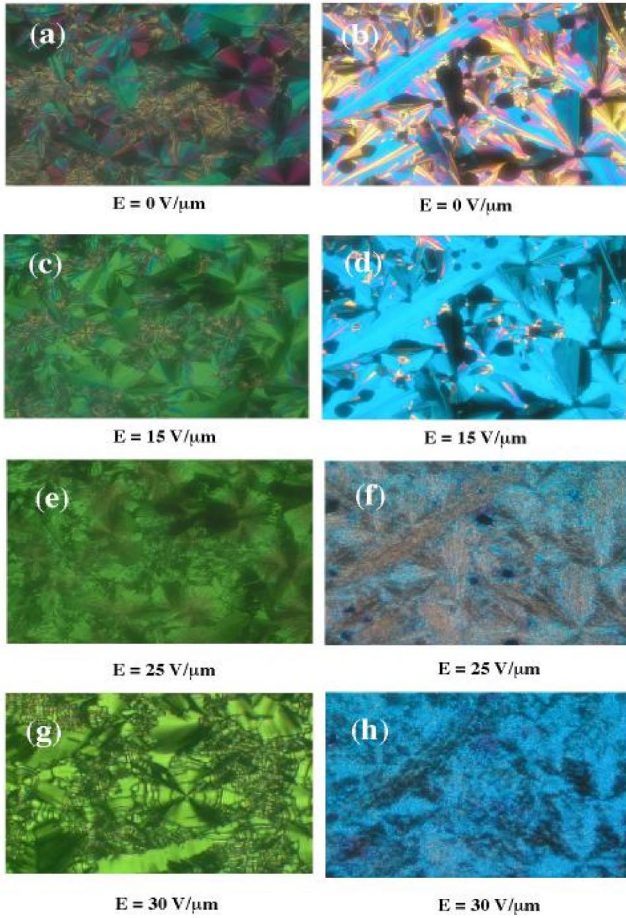
FIG. 3. (Color online) Textures of the studied compounds under different electric fields (square-wave field, 100 Hz). (a), (c), (e), and (g) correspond to the compound 1 and (b), (d), (f), and (h) to the compound 2. Under no field is a mosaic structure characteristic of the B_1 phase observed [(a) and (b)]. Under a field of 15 V μm^{-1}, the texture colors change to that corresponding to the maximum birefringence: (c) green for compound 1 ($\Delta n = 0.16$) and (d) blue for compound 2 ($\Delta n = 0.13$). At a field of 25 V μm^{-1}, a phase transition takes place [(e) and (f)]. Above that field, the phase is homochiral B_2 for both compounds [(g) and (h)]. The width of the photographs corresponding to compound 1 is 600 μm while that of compound 2 is 1200 μm.

microbeam diffraction experiments under electric field. This type of experiment is above our present capabilities. However, according to Ref. [16], the field-induced texture change is completely irreversible, and switching current is detected at the $B_{1\text{rev}}$ phase for fields higher than 15 V/μm, without changes in the optical texture. This is not the case with our compounds, which could indicate that we have a conventional B_1 phase but with the peculiarity of displaying a certain electro-optic response.

IV. ELECTRIC-FIELD-INDUCED PHASE TRANSITION

The texture transformation discussed up to now does not correspond to any structural change. However, on increasing the field further, a real phase transition takes place. This is evidenced by a drastic modification of the texture, passing

TABLE I. Indexing of the observed spacings and lattice parameters of the rectangular cell of the B_1 phase for the studied compounds. c corresponds approximately to the molecular length.

Compound	$h\ k\ l$	Observed spacing (Å)	Cell parameters (Å)
1	1 0 1	46.2	$a = 81.7\ c = 56.0$
	0 0 2	28.0	
	2 0 2	23.1	
2	1 0 1	43.8	$a = 79.7\ c = 52.4$
	0 0 2	26.0	
	1 0 3	17.2	

through an intermediate stage with a ''sandy'' texture and domain flow, usually meaning a deterioration of the material [Figs. 3(e) and 3(f)]. Nevertheless, the materials do not suffer any degradation. At even higher fields a steady texture develops, with larger domains and a birefringence similar to the maximum Δn found in the B_1 phase. Figures 3(g) and 3(h) show the new textures under square-wave fields of 30 V/μm and $\nu = 100$ Hz. In some areas of the samples, circular domains are still visible, but the extinction brushes are now oriented at about 45° from the polarizing directions [Figs. 5(a) and 5(b)]. This means that the new structures are syn-
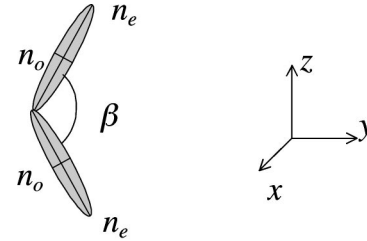
$$n_x = n_o$$

$$n_y = \left(n_o^2 \sin^2 \frac{\beta}{2} + n_e^2 \cos^2 \frac{\beta}{2} \right)^{1/2}$$

$$n_z = \left(n_o^2 \cos^2 \frac{\beta}{2} + n_e^2 \sin^2 \frac{\beta}{2} \right)^{1/2}$$

Compound	n_x	n_y	n_z	$n_z - n_y$	$\Delta n_{\min}$	$n_z - n_x$	$\Delta n_{\max}$
1	1.50	1.55	1.66	0.11	0.11	0.16	0.16
2	1.50	1.56	1.64	0.08	0.08	0.14	0.13

FIG. 4. Schematic representation of the approach used to calculate the refractive indices in the B_1 phase. The molecule can be assumed to be composed of two uniaxial wings making an angle β and with refractive indices n_e and n_o. The principal refractive indices of the B_1 phase are obtained by averaging the contribution of the wings. The calculated refractive indices for both compounds are presented in the table together with the calculated and measured ($\Delta n_{\min}$ and $\Delta n_{\max}$) birefringences.
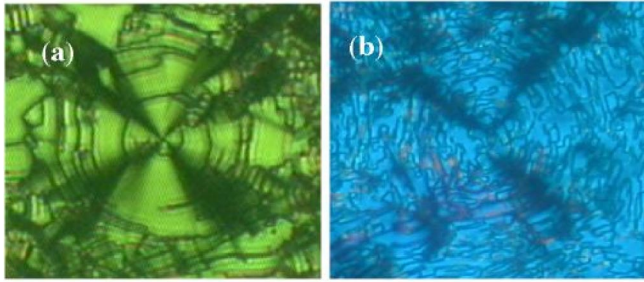
FIG. 5. (Color online) Details of the textures of the field-induced B_2 phase under an electric square-wave field of 30 V μm^{-1}, 100 Hz. (a) and (b) correspond to compounds 1 and 2, respectively. The extinction brushes are rotated an angle of about 45° in both pictures, which indicates a synclinic molecular arrangement in the B_2 phase. The width of the photographs corresponds to 150 μm.

clinic under the field and the tilt values are close to $\theta = 45°$. This special θ value prevents us from observing a texture change when the polarity of the field is reversed. However, the materials are in fact switching, as demonstrated in Fig. 6(a) for compound 1, where the polarization switching current under a triangular wave is shown. When the maximum field is around 20 V/μm, two well-separated small bumps per half period of the exciting wave arise. Increasing the field and coinciding with the appearance of the sandy texture, a third peak develops in between. For 30 V/μm, the current cycle exhibits a behavior typical of a smectic antiferroelectric phase. The material remains in the new phase during the whole period of the exciting wave. The peak's disposition is similar to that shown by the low-temperature phase as depicted in Fig. 6(b). In this figure, the switching current for two different temperatures is represented, one corresponding to the low-temperature phase and the other to the B_1 phase. At this point, it is interesting to comment that the transition temperatures in glass cells are different from those deduced from DSC measurements (the B_1 phase takes place between 159 °C and 130 °C). We have found this current response in the B_1 phase whenever the applied field is above the threshold that produces the sandy texture. In Fig. 7 we have plotted some critical fields versus temperature including the low- and high-temperature phases: E_{th} represents the field that induces the sandy texture in the B_1 phase and above which we observe switching; E_{AF} is the position of the current peak that corresponds to the antiferroelectric-ferroelectric transition and E_{FA} is the position of the peak that corresponds to the ferroelectric-antiferroelectric one (always triangular field, 50 Hz). Several points have to be remarked. E_{th} is quite large and decreases smoothly with temperature. E_{AF} and E_{FA} have a smooth behavior across the phase transition and even show a small decrease as temperature increases whenever the applied field is larger than E_{th} in the B_1 phase. We think that the B_1 phase under fields higher than E_{th} transforms into a B_2 phase (in the following paragraph we will give more evidence about this point), and the material remains in this phase while switching. This fact would also explain the similarity of the cycles in both mesophases.
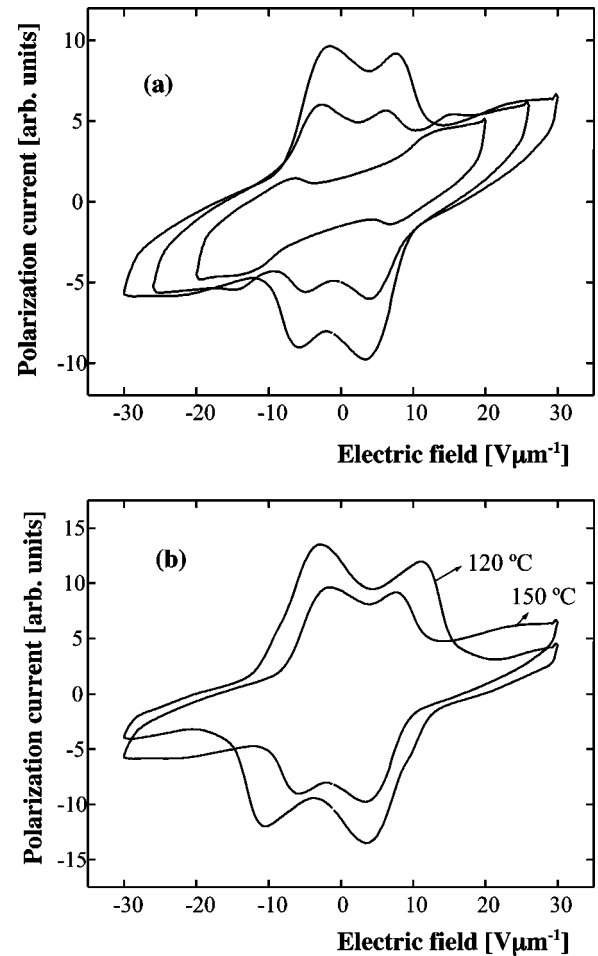
FIG. 6. Polarization switching current for compound 1 under a triangular-wave electric field of 50 Hz. (a) For different maximum field values in the high-temperature phase; (b) for the same electric field at two different temperatures corresponding to the high- and low-temperature phases.

Another evidence of the high-field phase identification as B_2 is based on the textures [Figs. 3(g), 3(h), 5(a), and 5(b)] typical of this structure. The identification is also consistent with the difficulty and relatively long time (a few seconds) that is necessary experimentally to complete the transformation from the B_1 phase. This seems logical since the B_1-B_2 transition involves a profound rearrangement of the phase because it requires a breaking of the close-packing B_1 structure and a subsequent formation of smectic layers.

There is still another fact supporting the identification as a B_2 phase. As will be shown next, the low-temperature phase of compound 1 is a B_2 phase, with the same texture under an electric field as that shown in Figs. 3(g) and 5(a). Figure 8 shows the texture of this phase. Under an applied field, the structure is SmC_SP_F, with the brushes tilted about 45° [Fig. 8(a)]. The remarkable dark color after field removal [Fig. 8(b)] is due to the fact that a tilt angle near 45° in a SmC_AP_A structure causes the material to be close to the orthoconic situation that provokes a drastic decrease of the birefringence [18]. The x-ray results are also compatible with this idea. Three low-angle reflections are observed in this phase, with
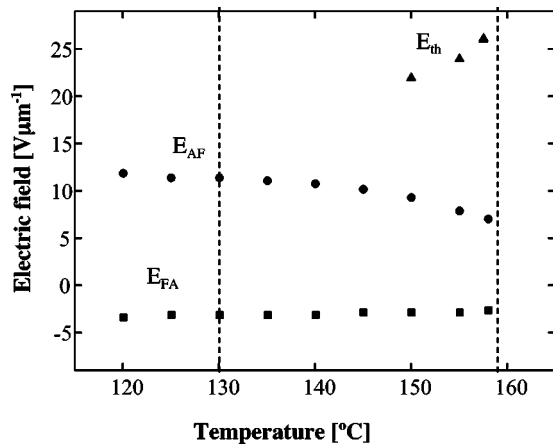
FIG. 7. Critical electric fields vs temperature for compound 1 (triangular-wave, 50 Hz). E_{th}: threshold field that induces the B_1-B_2 phase transition. E_{FA}: field at which the ferroelectric-antiferroelectric transition takes place. E_{AF}: field corresponds to the antiferroelectric-ferroelectric transition. The temperatures correspond to measures carried out in glass cells for which the high-temperature phase has been observed from 159 °C down to 130 °C. The vertical lines separate the I-B_1 and the B_1-B_2 regions for null electric field.

spacings 47.3, 23.7, and 16.0 Å, practically independent of temperature. These reflections can be explained in terms of a unique characteristic distance $d = 47.5$ Å, which corresponds to the smectic layer spacing of the B_2 phase, and would imply a molecular tilt of 41° assuming a rigid molecular model.

It would be of great interest to carry out x-ray measurements in order to state definitively the identification of the field-induced phase as B_2. Unfortunately, this experiment cannot be performed since the required high bias field is above the damage threshold of these materials.

V. DIELECTRIC MEASUREMENTS

Figures 9(a) and 9(b) are three-dimensional plots of the dielectric losses versus temperature and frequency for both compounds on cooling (EHC cells, $d = 7$ μm). The spectrum
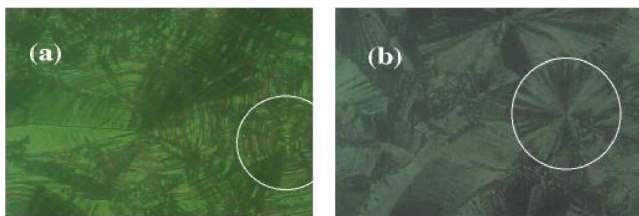
FIG. 8. (Color online) Textures of the B_2 phase of compound 1. Under electric field (a) the extinction brushes deviate for the polarizer-analyzer position about 45°. This texture is similar to that of the high-temperature phase under an electric field above E_{th}. After having removed the field (b) the brushes coincide with the polarizer-analyzer position due to the anticlinic arrangement of the molecules. The orientation of the extinction brushes appears clearly in the regions enclosed by the white circles. The width of the photographs corresponds to 250 μm.
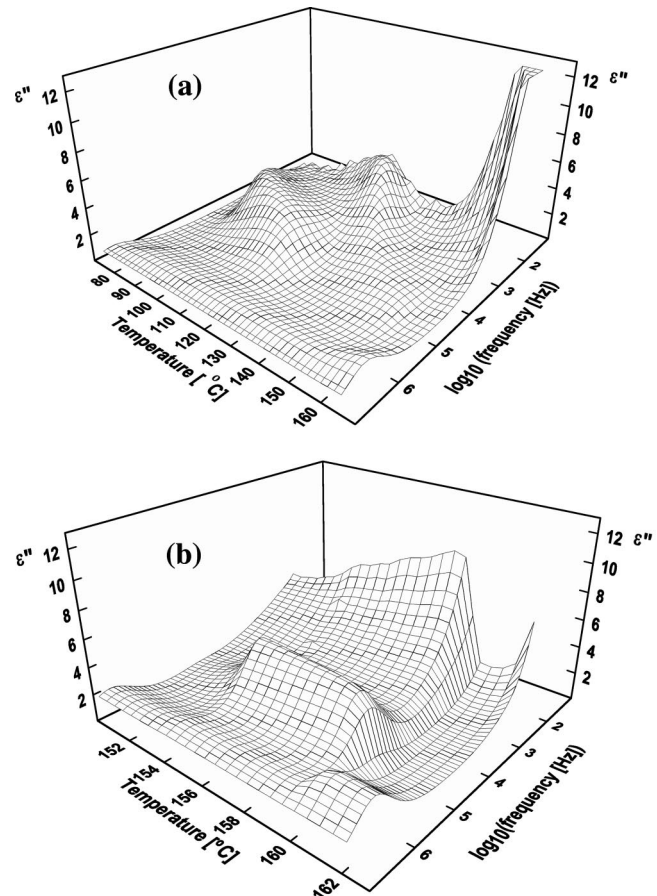
FIG. 9. 3D plots of the dielectric losses vs temperature and frequency for compound 1 (a) and 2 (b).

of the B_1 phase of compound 2 is dominated by a mode around 10^5 Hz [Fig. 9(b)]. For compound 1, a mode whose frequency is around 10^5 Hz near the I-B_1 transition is also present with a strong thermal activation [Fig. 9(a)]. At around 130 °C, coinciding with the appearance of some domains of the B_2 phase, a new relaxation mode at a larger frequency starts to appear. During several degrees, both modes are present. Figures 10(a) and 10(b) show, respectively, the frequencies and strengths versus temperature of the modes mentioned above.

In the most usual I-B_2 phase transition, the reported [19] dielectric behavior consists, basically, in a mode in both phases, whose frequency shows a jump at the transition. This mode is related to the rotation around the molecular long axis and then involves the transverse dipole moment, quite large for this type of compound. In the present case, in which an I-B_1 phase transition is present, the dielectric behavior has the same origin. We checked with metallic cells that the mode was also present in the I phases of our materials at around 10^7 Hz (it was not possible to use the glass cells for this purpose because of the spurious contribution at high frequencies of the finite resistivity of the ITO electrodes). In the B_2 phase of compound 1, a mode at a larger frequency than in the B_1 phase is present. We think that it is also related to the rotation around the molecular long axis, its frequency in the B_1 phase being smaller than that in the B_2 phase,
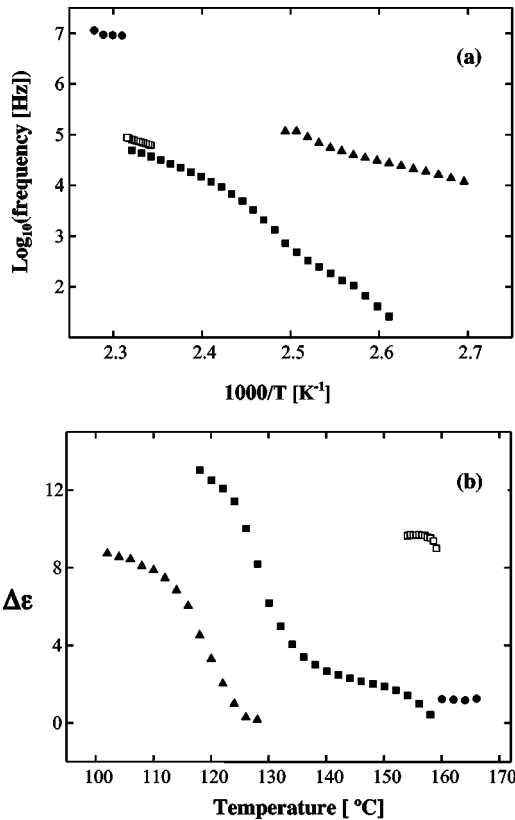
FIG. 10. Temperature behavior of the dielectric modes. (a) Arrhenius plot of the frequencies. (b) Dielectric strengths vs temperature. Solid and open symbols correspond to compounds 1 and 2, respectively. Circles, I phase; squares, B_1 phase; triangles, B_2 phase. For compound 1, a coexistence of the B_1 and B_2 phases can be observed in a wide temperature range.

probably due to the higher order of the short molecular axes. The presence of the low-frequency mode, coming from the B_1 phase, together with the one corresponding to the B_2 phase is understandable because there is phase coexistence. What is not that clear is its behavior versus temperature; the frequency quickly decreases while the strength increases, see Fig. 10(b). Probably this effect, due to the metastability of the B_1 phase, should imply a highly increasing tendency of the strength of the mode in this phase when lowering the temperature.

Finally, we would like to mention that the behavior of the dielectric permittivity corroborates part of our previous conclusions about the effect of high fields on the B_1 phase. For both compounds, the complex dielectric permittivity is simi-

lar in three situations: (a) For a virgin sample in the B_1 phase, Figs. 3(a) and 3(b); (b) upon removal of a field similar to that needed to obtain the texture of Figs. 3(c) and 3(d); (c) upon removal of a field larger than E_{th}.

The only difference is the strength of the mode: $\Delta\varepsilon_b > \Delta\varepsilon_a > \Delta\varepsilon_c$. This means that in (b) the sample is more ordered than in (a) being in (c) when more disordered, as the textures also suggest. It is also interesting to remark that although the texture (a) cannot be fully recovered after the application of a high enough field, the texture (b) can be reobtained from (c) just by applying an intermediate field, returning also the dielectric strength to the value obtained in (b). This means that the field effects are reversible and do not produce any damage to the sample.

VI. CONCLUSIONS

In summary, we have observed a B_1-B_2 transition induced by a low-frequency electric field in two materials. The required field is rather strong, $E_{th}=25$ V/μm, and the transition takes place through a profound molecular reorganization, involving the alignment of the dipoles and the formation of smectic layers with tilted molecules. The transition is reversible, though the size and shape of the B_1 domains change completely when the field is returned to zero. Once the B_2 phase is formed, the materials remain in this phase even when subjected to a triangular-wave field, provided that the amplitude is larger than E_{th} and the frequency above several Hz. Moreover, in this state the materials have switching characteristics typical of usual B_2 phases, with critical fields E_{AF} and E_{FA} of magnitude well below E_{th} and basically temperature-independent. This behavior of the threshold and critical fields resembles that found for the so-called general Sm-C (Sm-C_G) to B_2 transition [20]. In our case, however, this possibility is discarded given the observed textures and x-ray measurements in our high-temperature mesophases, which unambiguously point towards a B_1 phase. At the moment, we are unable to explain the molecular features that make these phases respond to the electric field.

[1] T. Niori, T. Sekine, J. Watanabe, T. Furukawa, and H. Takezoe, J. Mater. Chem. **6**, 1231 (1996).

[2] G. Pelzl, S. Diele, and W. Weissflog, Adv. Mater. (Weinheim, Ger.) **11**, 707 (1999).

[3] D.R. Link, G. Natale, R. Shao, J.E. Maclennan, N.A. Clark, E. Kórblova, and D.M. Walba, Science **278**, 1924 (1997).

[4] J. Watanabe, T. Niori, T. Sekine, and H. Takezoe, Jpn. J. Appl.

Phys., Part 2 **37**, L139 (1998).

[5] The precise molecular arrangement in the B_1 phase is still a subject of controversy. There is not complete evidence that the scheme of Fig. 1(b) is correct. Recent reports [6] seem to give more support to the model of Fig. 1(b′) for all the B_1 structures and even more complicated arrangements with molecular tilt and splay of the polarization have also been proposed by

Coleman *et al.* [7]. We will not discuss this problem here.

[6] K. Pelz, W. Weissflog, U. Baumeister, and S. Diele, Liq. Cryst. **30**, 1151 (2003).

[7] D.A. Coleman *et al.*, Science **301**, 1204 (2003).

[8] W. Weissflog, F. Wirth, S. Diele, G. Pelzl, H. Schmalfuss, T. Schoss, and A. Würflinger, Liq. Cryst. **28**, 1603 (2001).

[9] H.N. Shreenivasa Murthy and B.K. Sadashiva, Liq. Cryst. **29**, 1223 (2002).

[10] J.C. Rouillon, J.P. Marcerou, M. Laguerre, H.T. Nguyen, and M.F. Achard, J. Mater. Chem. **11**, 2946 (2001).

[11] G. Dantlgraber, D. Shen, S. Diele, and C. Tschierske, Chem. Mater. **14**, 1149 (2002).

[12] It could also imply a tilt of the molecular director with respect to the c axis of the structure. Such a possibility has been recently reported for several materials with the B_1 phase [13].

[13] J. Mieczkowski, K. Gomola, J. Koseska, D. Pociecha, J. Szydlowska, and E. Gorecka, J. Mater. Chem. **13**, 2132 (2003).

[14] In the case of a tilted B_1 phase, the orientation of the extinction brushes would imply that the molecular tilt is opposite for the columns with opposite polarization.

[15] All the possibilities of nontilted columnar rectangular phases are also compatible with the observed textures and exhibit the same values of the birefringence.

[16] J. Szydlowska, J. Mieczkowski, J. Matraszek, D.W. Bruce, E. Gorecka, D. Pociecha, and D. Guillon, Phys. Rev. E **67**, 031702 (2003).

[17] Y. Takanishi, T. Izumi, J. Watanabe, K. Ishikawa, H. Takezoe, and A. Iida, J. Mater. Chem. **9**, 2771 (1999).

[18] K. D'have, P. Rudquist, S.T. Lagerwall, H. Pauwels, W. Drzewinski, and R. Dabrowski, Appl. Phys. Lett. **76**, 3528 (2000).

[19] H. Kresse, H. Schlacken, U. Dunemann, M.W. Schröder, G. Pelzl, and W. Weissflog, Liq. Cryst. **29**, 1509 (2002).

[20] A. Eremin, S. Diele, G. Pelzl, H. Nádasi, and W. Weissflog, Phys. Rev. E **67**, 021702 (2003).